

Monte Carlo calculations of positron emitter yields in proton radiotherapy

This article has been downloaded from IOPscience. Please scroll down to see the full text article.

2012 Phys. Med. Biol. 57 1659

(<http://iopscience.iop.org/0031-9155/57/6/1659>)

View [the table of contents for this issue](#), or go to the [journal homepage](#) for more

Download details:

IP Address: 109.232.42.33

The article was downloaded on 07/03/2012 at 16:02

Please note that [terms and conditions apply](#).

Monte Carlo calculations of positron emitter yields in proton radiotherapy

E Seravalli¹, C Robert^{2,9}, J Bauer^{3,9}, F Stichelbaut^{4,9}, C Kurz^{3,9},
J Smeets⁵, C Van Ngoc Ty⁶, D R Schaart⁷, I Buvat², K Parodi³
and F Verhaegen^{1,8,10}

¹ Department of Radiation Oncology (MAASTRO), University Medical Centre Maastricht, Maastricht, The Netherlands

² IMNC—UMR 8165 CNRS, Universités Paris 7 et Paris 11, Bât 440, Orsay, France

³ Heidelberg Ion Beam Therapy Centre and Department of Radiation Oncology, Heidelberg University, Clinic, Heidelberg, Germany

⁴ IBA, Louvain-la-Neuve, Belgium

⁵ Service de Métrologie Nucléaire, Université Libre de Bruxelles

⁶ CEA-SHFJ, Orsay, France

⁷ Delft University of Technology, Delft, The Netherlands

⁸ Department of Oncology, McGill University, Montréal, Québec H3G 1A4, Canada

E-mail: frank.verhaegen@maastro.nl

Received 8 December 2011, in final form 22 January 2012

Published 7 March 2012

Online at stacks.iop.org/PMB/57/1659

Abstract

Positron emission tomography (PET) is a promising tool for monitoring the three-dimensional dose distribution in charged particle radiotherapy. PET imaging during or shortly after proton treatment is based on the detection of annihilation photons following the β^+ -decay of radionuclides resulting from nuclear reactions in the irradiated tissue. Therapy monitoring is achieved by comparing the measured spatial distribution of irradiation-induced β^+ -activity with the predicted distribution based on the treatment plan. The accuracy of the calculated distribution depends on the correctness of the computational models, implemented in the employed Monte Carlo (MC) codes that describe the interactions of the charged particle beam with matter and the production of radionuclides and secondary particles. However, no well-established theoretical models exist for predicting the nuclear interactions and so phenomenological models are typically used based on parameters derived from experimental data. Unfortunately, the experimental data presently available are insufficient to validate such phenomenological hadronic interaction models. Hence, a comparison among the models used by the different MC packages is desirable. In this work, starting from a common geometry, we compare the performances of MCNPX, GATE and PHITS MC codes in predicting the amount and spatial distribution of proton-induced activity, at therapeutic energies, to the already

⁹ These authors contributed equally to the paper.

¹⁰ Author to whom any correspondence should be addressed.

experimentally validated PET modelling based on the FLUKA MC code. In particular, we show how the amount of β^+ -emitters produced in tissue-like media depends on the physics model and cross-sectional data used to describe the proton nuclear interactions, thus calling for future experimental campaigns aiming at supporting improvements of MC modelling for clinical application of PET monitoring.

(Some figures may appear in colour only in the online journal)

1. Introduction

Monte Carlo (MC) simulation codes of radiation transport are increasingly becoming essential tools in charged particle therapy. They can describe the complex physics of charged particle interactions and, in general, all aspects of radiation interaction with matter. At the same time, they provide accurate multi-dimensional particle transport and account for complex geometries, such as fully detailed CT-based descriptions of the patient anatomy (Carlsson *et al* 1997, Parodi *et al* 2007b, Paganetti *et al* 2008).

Whereas electromagnetic interactions responsible for the ion energy transfer and related dose deposition are sufficiently well known and reliably described, the modelling of nuclear interactions is affected by significant uncertainties since there is no exact physical model available. Different phenomenological approaches have been proposed and several MC codes, with different implementations of physics and tracking, are available to the user. These phenomenological approaches often have limitations and in general it is impossible, for a given model, to ensure a uniform level of accuracy in comparison with existing experimental data for all observables of interest. Therefore, it is of utmost importance to compare the results obtained with different MC codes in the context of the intended application.

The purpose of this work is to compare the performances of four MC packages for the prediction of proton-induced β^+ -activity distribution. The detection of annihilation photons following the β^+ -decay of radionuclides resulting from nuclear reactions in the irradiated tissue by positron emission tomography (PET) imaging has been demonstrated to be a promising tool for the three-dimensional monitoring of the dose distribution in charged particle beams (Parodi *et al* 2002, 2005, 2007b, Attanasi *et al* 2011). Therapy monitoring is achieved by comparing the measured and pre-calculated β^+ -activity distributions. In this approach, the accuracy of the calculated activity distribution depends on the accuracy of the employed MC code.

We compare three MC codes, MCNPX, GATE and PHITS, to the already experimentally validated and clinically used PET modelling based on the FLUKA code combined with experimental cross sections (Parodi *et al* 2005, 2007a, 2007b, 2007c). Uncertainties for this method are in the order of 10%–15% as quoted in Parodi *et al* (2002, 2005).

It is noted that all the codes investigated here have already been used for charged particle therapy applications and that some validations against available experimental data have been published (Stankovskiy *et al* 2009, Herault *et al* 2005, Pshenichnov *et al* 2006, Paganetti and Gottschalk 2003, Paganetti *et al* 2008, Parodi *et al* 2009, Rinaldi *et al* 2011, Grevillot *et al* 2011, Jan *et al* 2011, Zahra *et al* 2010, Iwase *et al* 2006, Nose *et al* 2005).

In this work, starting from a common setup, we compare depth–dose curves, proton fluence and the production rates for ^{11}C and ^{15}O ions, as these two isotopes are the most abundant positron emitters produced in proton irradiation of human tissue (Beebe-Wang *et al* 2003).

2. Methods and materials

Four MC packages have been investigated: MCNPX (section 2.1.1), GATE (section 2.1.2), PHITS (section 2.1.3) and FLUKA (section 2.1.4). A common geometry, described in section 2.2, was chosen to make the comparison among codes independent of the initial simulation setup, thus enhancing the different characteristics of the MC codes. For the same reason, simulations were performed for monoenergetic infinitely narrow pencil beams.

2.1. Brief description of the MC codes

2.1.1. MCNPX. MCNPX (<http://mcnpx.lanl.gov>) is a radiation transport code developed at Los Alamos National Laboratory (LANL) and capable of tracking many particle types (electron, photons, nucleons and light ions) and heavy ions over a wide range of energies (MCNPX 2008). MCNPX uses (1) standard evaluated nuclear data tables to transport protons and neutrons; (2) physics models to transport additional particle types such as deuterons, tritons, alphas, pions, muons, etc and (3) physics models to transport neutrons and protons when no tabular data are available.

The proton transport algorithms take into account energy straggling, multiple Coulomb scattering, elastic and inelastic scattering and nonelastic nuclear interactions (MCNPX 2008). The use of the collision energy-loss model (maximum kinetic energy transfer model) leads to stopping powers in close agreement with ICRU data (MCNPX 2002). The implemented multiple-scattering model relies on Rossi's theory, assuming a Gaussian distribution of angular deflections (Herault *et al* 2005, MCNPX 2002, Sawakuchi *et al* 2010).

In this work, MCNPX 2.7D has been used together with the LA150 cross-sectional library (Chadwick *et al* 1999) whenever available for the transported particles, and the Cascade-Exciton model (CEM) (Mashnik 2006), as suggested by the developers (Waters 2010), otherwise (e.g., for protons with energies >150 MeV).

In version 2.7D, the possibility of changing the transport step size for protons (stopping power table energy binning) (MCNPX 2010) has been implemented allowing for smooth dose distributions. The deposited energy per unit mass (tally type 6) was used to score absorbed dose while for scoring fluence, tally type 1 was used. In order to extract the ^{11}C and ^{15}O cross sections from the CEM internal model, the routines *xsex3* and *htapex3* were employed (MCNPX 2008). For scoring the production rates of ^{11}C and ^{15}O , proton fluences were combined with experimental or internal model cross sections (section 2.2) using a tally type 4 (track length estimate of particle flux) together with an energy-dependent response function (cf pp 5–112 of the MCNPX 2.6 manual (MCNPX 2008)).

2.1.2. GATE. GATE version 6 (Jan *et al* 2011) (www.opengatecollaboration.org) is an MC simulation application enabling modelling of emission tomography, transmission tomography and radiation therapy. GATE is based on the GEANT4 toolbox (Agostinelli *et al* 2003). In this work, GATE version 6.1 based on GEANT4 version 9.4 was used. As recommended by the GEANT4 Electromagnetic Standard working group, the Opt3 electromagnetic standard package parameters were selected (see table A1 in the appendix). A fine sampling of the cross-sectional tables (20 bins per decade) as well as 0.1 mm (e^-) and 0 mm (proton) production cut values were used for improved accuracy. A modified version (removal of the calls to the precompound model) of the GEANT4 Binary Cascade (BC) model was used for the primary protons. For neutrons, the BC model was used for energies larger than 14 MeV. The high precision neutron package (NeutronHP) was used to transport neutrons down to thermal energies. Table A2 in the appendix summarizes the models implemented in the simulations.

In GATE, actors are tools enabling the collection of information during the simulations. For this study, the DoseActor was used to record the energy and dose distributions as a function of depth. The ProductionAndStoppingActor was used to record the ^{11}C and ^{15}O distributions. The proton fluence was obtained using the EnergySpectrumActor.

2.1.3. PHITS. PHITS is a general-purpose particle and heavy-ion transport code system used in various research fields such as radiation science, accelerator shielding design, medical applications, space research, etc (Iwase *et al* 2006, Nose *et al* 2005). It uses two simulation codes Jet AA microscopic transport model (JAM) (Nara *et al* 2000) and JAERI quantum molecular dynamics (JQMD) (Niita *et al* 1995) to describe intermediate and high-energy nuclear reactions. The JQMD code is based on the quantum molecular dynamics model and has been widely used to study various aspects of nucleon-induced reactions and heavy-ion interactions.

The PHITS code models the transport in materials of all particles (electrons, photons, nucleons, nuclei and mesons) over wide energy ranges, using nuclear data libraries and nuclear reaction models. Below 10 MeV/n, only the ionization process for the nucleus transport is taken into account. Above 10 MeV/n and up to 100 GeV/n, the nucleus–nucleus interactions are described by JQMD. Both JQMD and JAM can be used to describe the dynamic stage of the reactions, while the generalized evaporation model (Furihata 2000) is used for light particle evaporation and fission process of the excited residual nuclei. Between 0.1 and 20 MeV, neutrons are described in the same manner as in the MCNP4C code based on evaluated nuclear data such as the ENDF-B/VI, JENDL-3.3 and LA150 libraries. The simulation model JAM is used for neutron-induced reactions above 20 MeV. PHITS also uses evaluated nuclear data for photon and electron transport in the same manner as the MCNP4C code. For protons and other hadrons, JAM is also used above 1 MeV up to 200 GeV. Below 1 MeV, only the ionization process is considered until the charged particles are stopped.

The average stopping power for the charged particles and nuclei is computed using either the SPAR code (Armstrong and Chandler 1973) or the ATIMA package developed at GSI (Scheidenberger and Geissel 1998). For the angular straggling, the user can select among three different parameterizations: (1) the original Coulomb diffusion, (2) the first order of the Molière model and (3) the ATIMA model.

The total nucleus–nucleus reaction cross section used to determine the mean free path of the transported particles is based upon either the Shen formula (Shen *et al* 1989) or the NASA parameterization developed by Tripathi *et al* (1999). For this study, version 2.23 of PHITS (PHITS 2001) was used.

2.1.4. FLUKA. FLUKA (www.fluka.org) is a general-purpose MC package for calculations of particle transport and interactions with matter, widely used for an extended range of applications including activation, dosimetry and particle therapy (Battistoni *et al* 2007, Ferrari *et al* 2005).

The simulations presented in this work were performed with the FLUKA version 2011.2.2, applying the recommended default settings for hadrontherapy (*HADROTHER*) providing a detailed description of the complete transport of the primary protons and the produced secondary particles.

In FLUKA, inelastic interactions are handled by dedicated models covering different types and energy regimes. Nucleus–nucleus interaction at energies between 0.1 and 5 GeV per nucleon are treated by the relativistic quantum molecular dynamics model, while the Boltzmann master equation modelling is employed for an appropriate handling of interactions

Table 1. Ionization potential values used by the four MC codes for the simulations. Data taken from NIST (<http://physics.nist.gov/PhysRefData/Star/Text/PSTAR.html>) are reported for comparison.

Ionization potential (eV)	GATE	MCNPX	FLUKA	PHITS	NIST
Water	75	75	75	75	75
PMMA	74	71	74	71	74

below an energy of 0.1 GeV/ n down to the Coulomb barrier (Cerutti *et al* 2006). Inelastic hadron–nucleus interactions up to 5 GeV are described by pre-equilibrium approach to nuclear thermalization (Ferrari and Sala 1998).

With the hadron therapy default settings, the particle transport threshold is set to 0.1 MeV, except for neutrons being transported down to thermal energies with a multi-group processing similar to MCNPX and PHITS. Precise modelling of the particle slowing down process is achieved by restricting the fraction of kinetic energy lost per step to 2%, taking into account ionization fluctuations as well as the production of delta rays above an energy of 100 keV. Furthermore, the latest evaporation model for heavy fragments was activated (cf ‘*PHYSICS*’ card).

The scoring of the energy deposition and the proton fluence in the target volume was performed by means of ‘*USRBIN*’ cards applying the common binning setup of this study. Simulation of the production of the β^+ -active isotopes ^{15}O and ^{11}C via the respective (p, pn) reaction channel (inclusive (p, d)) on oxygen and carbon target nuclei, respectively, was accomplished by the method described in Parodi *et al* (2002, 2007b) and introduced in the following as EXP (see section 2.2). This method employs the FLUKA user routine ‘*fluscw.f*’ to combine the energy-dependent proton fluence with experimental cross-sectional data, yielding USRBIN scoring volumes containing the spatial distribution of the considered β^+ -emitting isotope.

2.2. Simulation setup and scored quantities

Monoenergetic infinitely narrow proton pencil beams (10^6 protons) of 90, 160 and 200 MeV were used to irradiate a 35 cm long cylindrical volume (radius $r = 15$ cm) filled with water (mass density of 1.0 g cm^{-3}) or PMMA (mass density of 1.19 g cm^{-3}). Proton fluences and depth–dose curves were scored along the main cylinder axis, coinciding with the beam direction, with 0.05 mm sampling in depth and laterally integrated over the full radius of the phantom.

Yields of ^{11}C and ^{15}O were calculated for the main reaction channels using either the internal models of the codes or by combining cross sections and proton fluence according to the calculation approach described in Parodi *et al* (2007b). This procedure so far provided satisfactory agreement between simulations and experimental data for phantom investigations with the monoenergetic and spread-out proton Bragg peaks as well as for first clinical studies (Parodi *et al* 2007a). In this work, the experimental cross-sectional data sets (EXP) used by Parodi *et al* (2002) have been considered together with computed cross sections by means of the TALYS code (TENDL) (Talys 2010).

Table 1 depicts the ionization potential values implemented in the different codes. For water, the same ionization potential value is used by the investigated codes, while the value for PMMA employed by MCNPX and PHITS differs from the GATE and FLUKA one and recommended by NIST. In MCNPX, it is not possible to change the ionization potential value without recompiling the code. Recompiling the code is not trivial. Procedures on how to change the ionization potential and how to recompile the code are not indicated in this manual.

Table 2. Range prediction obtained from the four MC codes. Data taken from NIST (<http://physics.nist.gov/PhysRefData/Star/Text/PSTAR.html>) are reported for comparison. The range is defined as the position of the 90% level of the distal falloff.

Range (mm)	FLUKA	GATE	MCNPX	PHITS	NIST
Water—90 MeV	63.8	64.0	63.5	63.0	64.0
Water—160 MeV	176.3	176.5	176.0	175.00	176.5
Water—200 MeV	258.8	259.5	258.5	258.50	259.6
PMMA—90 MeV	54.8	54.5	54.5	53.5	55.2
PMMA—160 MeV	151.8	152.0	151.0	149.5	152.4
PMMA—200 MeV	223.3	223.5	221.5	220.5	224.1

In PHITS, the ionization potential can be changed by the user only for water, while for other materials it is internally computed on the basis of the known constituents. In GATE, the default ionization potential calculated by means of Bragg's additivity rule can be edited by the user. In FLUKA, the internal calculations of the ionization potential can be overwritten by the user directly providing the desired value to be used (cf card 'MAT-PROP' in the FLUKA manual).

3. Results

3.1. Depth–dose profiles and range prediction

Table 2 lists the range prediction, defined as the position of the 90% level of the distal dose falloff according to Bortfeld (1997), obtained from the four MC codes for different materials and beam energies. Data from NIST (<http://physics.nist.gov/PhysRefData/Star/Text/PSTAR.html>) are shown as reference.

Figure 1 shows the depth–dose curves in PMMA simulated by means of the four codes for the three investigated energies. In figure 2, deviations from the FLUKA depth–dose curve values are depicted. Deviations are calculated between 0 mm and the proton range to discard the Bragg peak tail deviations. The largest differences (up to 5% for GATE, 8% for MCNPX and 15% for PHITS) are observed around the Bragg peak. The structure visible in the MCNPX deviations at ~16 mm for 160 MeV and at ~86 mm for 200 MeV can be probably explained by the switch that is internally occurring in the code (for proton energies < 150 MeV) from the CEM internal model to the evaluated proton data library to calculate the proton energy loss.

3.2. Proton fluence

In figure 3, the proton fluence as a function of depth in the PMMA phantom as obtained from the four codes is presented for three different energies. Results for water are similar.

3.3. Production yields of ^{11}C and ^{15}O

In figure 4, different cross-sectional data sets for the $^{12}\text{C}(\text{p},\text{x})^{11}\text{C}$ and $^{16}\text{O}(\text{p},\text{x})^{15}\text{O}$ reaction channels are presented: (1) experimental set (EXP) used by Parodi *et al* (2002), (2) TENDL-2010 (TENDL) set (Talys 2010), (3) set produced by the MCNPX CEM internal model (CEM) and (4) the ICRU report 63 set (ICRU 2000) shown for comparison. The EXP cross sections consist of a collection of measured data, while the other data sets are derived theoretically.

Differently from the EXP data set relative to $^{12}\text{C}(\text{p},\text{pn})^{11}\text{C}$, the TENDL and the internal model cross sections also include the reaction channel $^{16}\text{O}(\text{p},3\text{p}3\text{n})^{11}\text{C}$. The latter reaction channel has three orders of magnitude lower cross section, for the considered energy range,

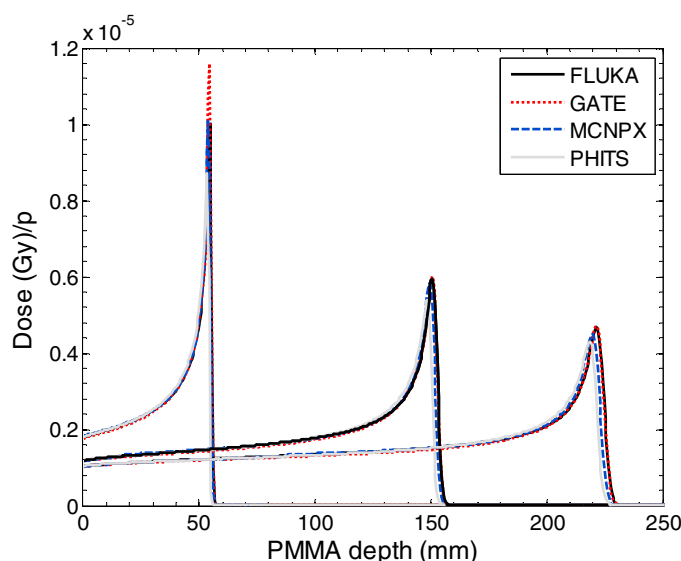


Figure 1. Simulated depth–dose curves in PMMA obtained from the four codes for 90, 160 and 200 MeV monoenergetic proton pencil beams. On the vertical axis, dose per initial proton hitting the target is shown. Black solid line refers to FLUKA, dotted line to GATE, dashed line to MCNPX and grey solid line to PHITS.

compared to the $^{12}\text{C}(p,pn)^{11}\text{C}$ cross-sectional magnitude (Beebe-Wang *et al* 2003). Therefore, having included the contribution coming from ^{16}O in the ^{11}C yield, when using the internal models, is expected to have a small impact on the comparison of yields obtained from EXP and theoretical data sets. This contribution was also neglected in Parodi *et al* (2002) where the first comparison of the β^+ -emitters yields calculated using the EXP cross sections against experimental data is shown.

The production cross-sectional data sets are very different as already observed by Beebe-Wang *et al* (2003) and Parodi *et al* (2005). Differences up to several tens of mb depending on the considered energy were noted.

Depth distributions of ^{11}C and ^{15}O production sites strongly depend on the cross-sectional data set that is used when convolving the proton fluence with the cross-sectional values, as can be seen in figure 5 for positron emitter distributions obtained with MCNPX for the EXP, TENDL and CEM cross-sectional data sets (160 MeV protons). The depth profiles differ in magnitude and shape. In the case of ^{11}C , a difference is also noted in the falloff of the profile when using the CEM and TENDL data set with respect to the profile obtained when using the EXP cross sections.

The positron emitter distributions calculated using the four MC codes and the experimental cross sections (EXP) are shown in figure 6. The shape and magnitude of the depth profiles agree fairly well. The distal falloff position discrepancies are consistent with the observed range variations in the depth–dose curves and fluences. The positron emitter depth profiles obtained with the internal models of GATE, MCNPX and PHITS for a 160 MeV monoenergetic pencil beam are represented in figure 7 in comparison to the approach using FLUKA with experimental cross sections (chosen as reference in this study). The depth profiles differ substantially from the profile obtained using the EXP cross-sectional data set. Similar differences among the isotope depth profiles were observed for 90 and 200 MeV, respectively.

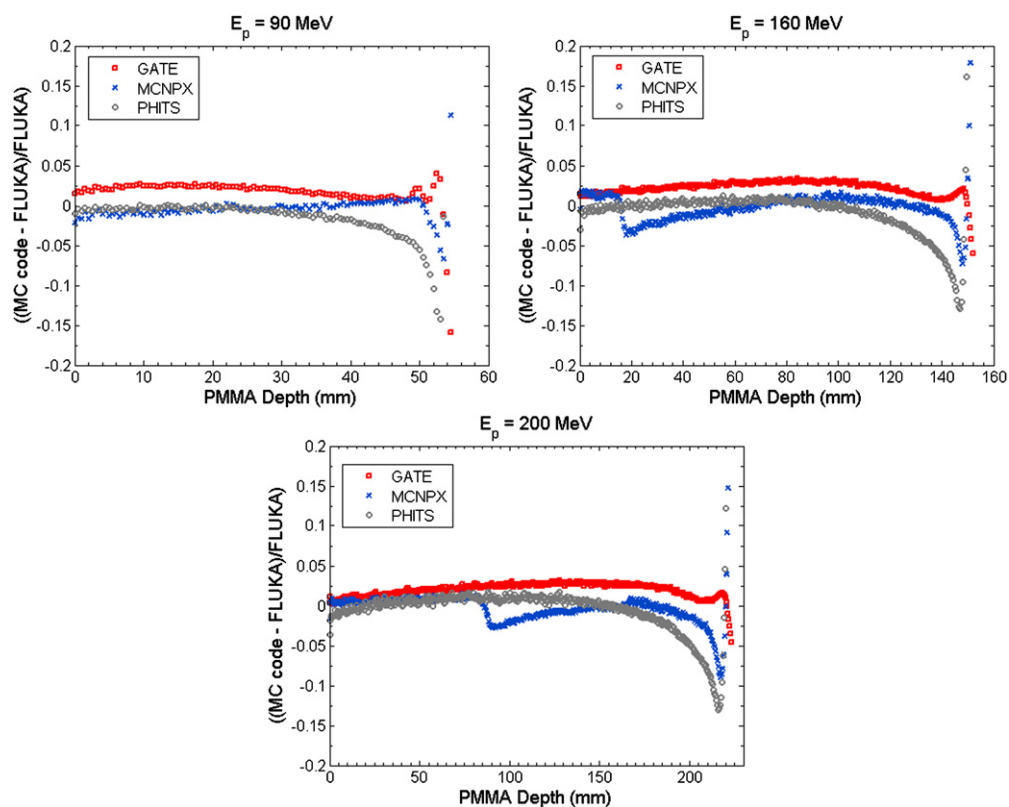


Figure 2. Differences of the depth–dose curve values simulated with GATE, MCNPX and PHITS with respect to FLUKA. Differences are calculated between 0 mm and the proton range to discard the Bragg peak tail deviations. Squares refer to GATE deviations, crosses to MCNPX deviations and dots to PHITS deviations.

Table 3. Total yields of ^{11}C and ^{15}O (per incident particle) produced by a 160 MeV monoenergetic proton pencil beam in a PMMA target computed using the four MC codes with the experimental (EXP) and the internal models (Int. Mod.) cross section. FLUKA results were extrapolated from the data presented in Parodi and Enghardt (2000) by assuming a linear dependence of the isotope yield on beam range.

	^{11}C (reactions/p)		^{15}O (reactions/p)	
	EXP	Int. Mod.	EXP	Int. Mod.
FLUKA	0.032	0.032	0.011	0.015
GATE	0.032	0.034	0.011	0.013
MCNPX	0.031	0.015	0.011	0.009
PHITS	0.030	0.013	0.010	0.005

Data showing results for the internal model of FLUKA can be found in Parodi and Enghardt (2000, 2002). Table 3 presents the ^{11}C and ^{15}O yields calculated for a 160 MeV monoenergetic proton pencil beam in the PMMA target using the experimental cross sections (EXP) and the internal models of the MC codes.

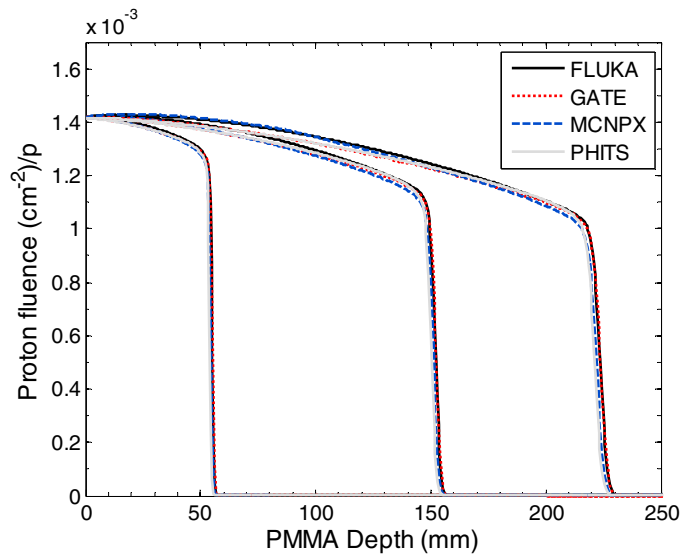


Figure 3. Proton fluence versus depth in the PMMA phantom for 90, 160 and 200 MeV monoenergetic proton pencil beam obtained from the four MC codes. On the vertical axis, proton fluence per initial proton hitting the target is represented.

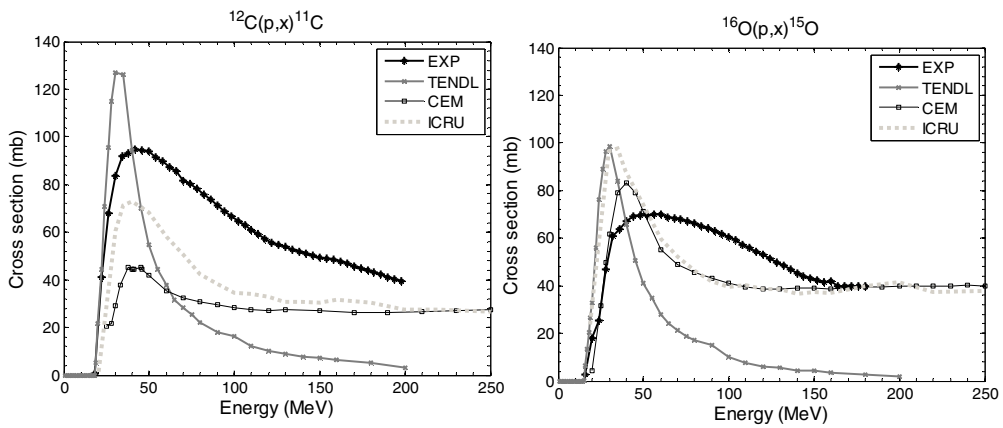


Figure 4. Nuclear reaction cross sections of $^{12}\text{C}(p,x)^{11}\text{C}$ (left) and $^{16}\text{O}(p,x)^{15}\text{O}$ (right). The data taken from four different sources are presented for comparison. For details, see legend and text.

4. Discussion

The range predictions by FLUKA and GATE in water and PMMA agree with the NIST values within 1 mm. Differences up to 1–1.5 mm are observed between the MCNPX and PHITS simulated range values in water and the corresponding NIST values. In PMMA, the MCNPX and PHITS range predictions show larger discrepancies: up to 3 mm for MCNPX and up to 4.5 mm for PHITS for the highest energy. These differences can be mainly attributed to the ionization potentials used by the MC codes (table 1) as already outlined by Andreo (2009).

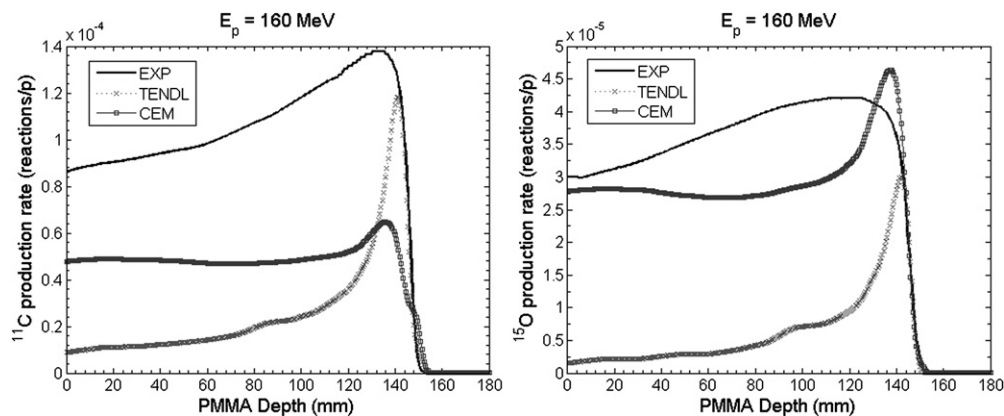


Figure 5. Yields of ^{11}C and ^{15}O versus depth produced by a 160 MeV monoenergetic proton pencil beam in a PMMA target computed with MCNPX using the EXP (solid line), TENDL (line with crosses) and CEM (grey line) internal model cross-sectional data sets. On the vertical axis, reactions per primary proton hitting the phantom are shown.

A consensus value of the ionization potential to be used by all the MC codes would seem advisable in order to get more consistent results. Moreover, more work is needed to improve our knowledge on ionization potential values.

Minor differences can be seen among the proton fluence predictions in water and PMMA obtained with the different MC codes, consistent with previous findings reported in Parodi *et al* (2007c) for previous versions of the Geant4 and FLUKA codes and consistent with the fact that the depth–dose curves were also found to be very similar.

From figures 5, 6, 7 and table 3, it can be concluded that the positron emitter quantitative yields and their depth profiles depend strongly on the cross-sectional data set used as already pointed out by Espana *et al* (2011), Beebe-Wang *et al* (2003) and Parodi *et al* (2005). If the same cross-sectional data set is used (i.e. EXP), then the depth profiles and yields computed by the MC codes are comparable.

Differences up to 6% and 9% are observed, respectively, for the ^{11}C and ^{15}O yields. On the other hand, when using the internal models of the codes, considerably different results are obtained. This is especially the case for the internal models of MCNPX and PHITS, systematically underestimating positron emitter production yields for both ^{16}O and ^{11}C (cf table 3). This indicates that the hadron interaction models used by the investigated codes cannot provide the same level of accuracy in comparison with existing experimental data for the observables of interest. In view of these findings, we suggest to use the experimental cross sections validated—and possibly fine tuned—against measured activation data taken at the specific PET scanner and facility-dependent beam line where PET monitoring is to be performed.

Finally, it should be noted that this study has concentrated on depth profiles, as these correlate with the proton beam range which is the quantity of major interest for PET-based *in vivo* treatment verification. Future investigations will address the accuracy of the MC codes for calculation of the lateral beam spreading in different materials, as inconsistencies of lateral dose calculations were pointed out by recent studies (Grevillot *et al* 2010, Kimstrand *et al* 2008) which might be of great relevance in view of proton beam scanning applications.

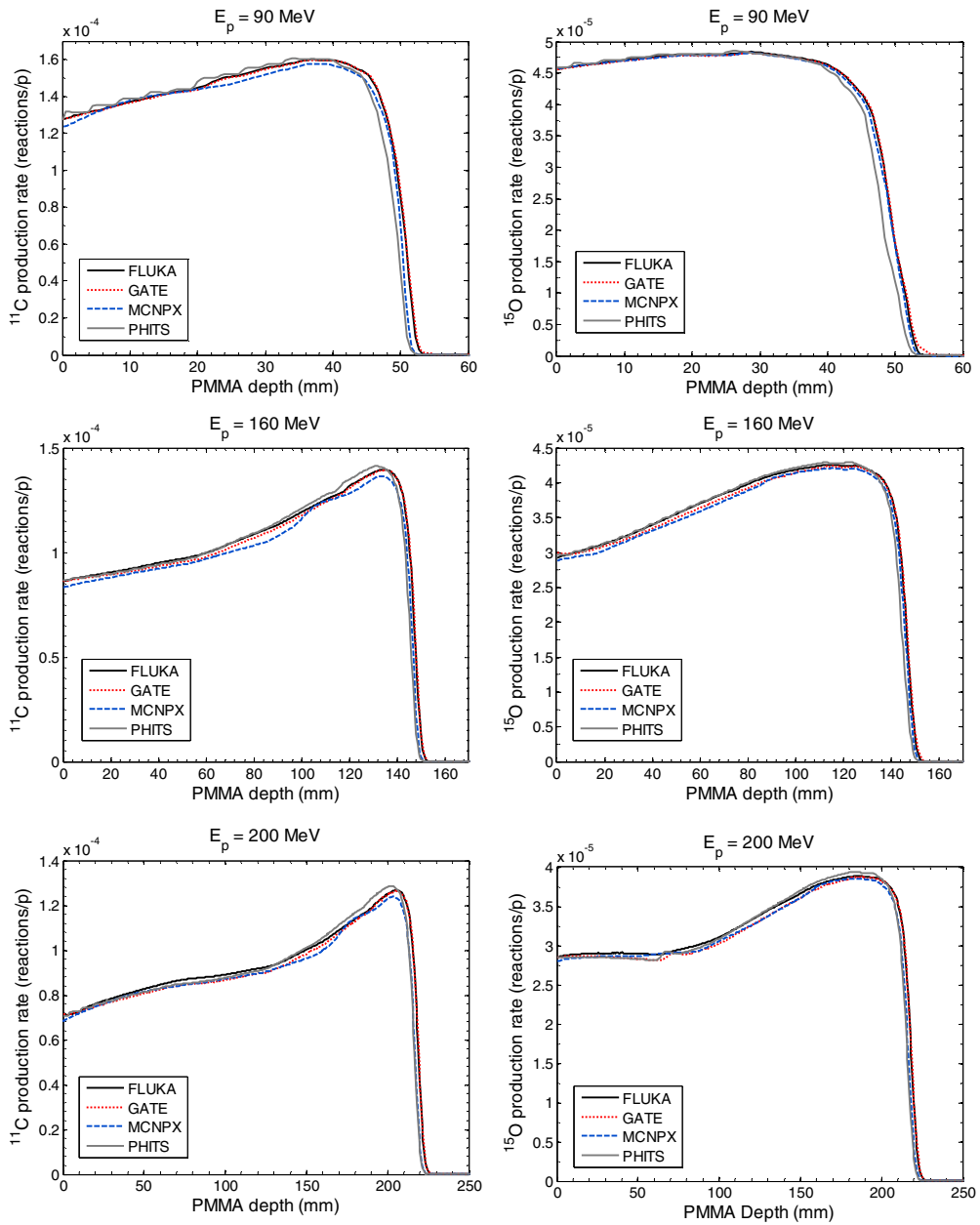


Figure 6. Yields of ^{11}C and ^{15}O versus depth produced by 90 and 200 MeV monoenergetic proton pencil beam in a PMMA target computed with the four MC codes for the EXP cross-sectional data set.

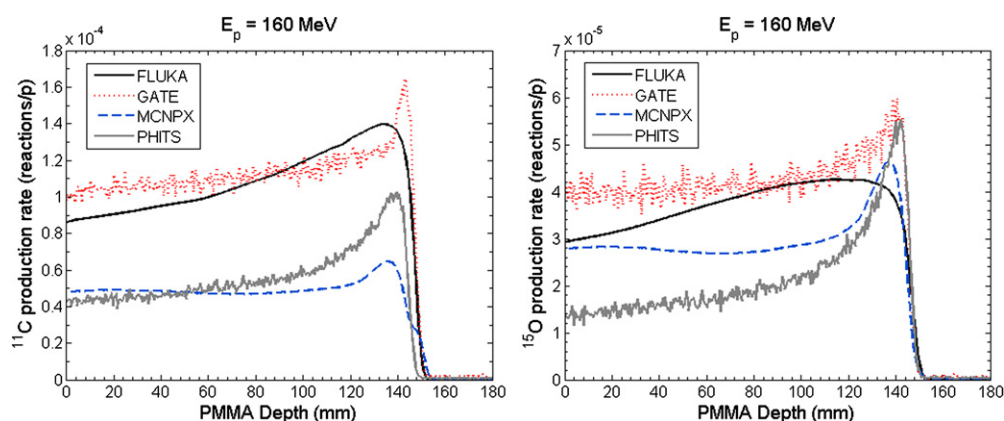


Figure 7. Yields of ^{11}C and ^{15}O versus depth produced by a 160 MeV monoenergetic proton pencil beam in a PMMA target computed using the internal models of GATE, MCNPX and PHITS. Yields of ^{11}C and ^{15}O versus depth obtained with FLUKA using EXP cross sections are shown for comparison.

5. Conclusions

We have compared the results of four MC codes used in hadron therapy, focusing in particular on the prediction of the β^+ -emitters produced during proton irradiation. The latter is important for PET-based verification of dose distributions delivered by charged particles.

It has been found that depth–dose curves, range prediction and proton fluence in water and PMMA homogenous phantoms simulated by the four MC codes show good overall agreement.

The internal phenomenological models of the MC codes produce positron emitter yields and depth profiles that are quite different from the ones obtained when using the experimental cross-sectional data. Therefore, there is a clear need for experimental data to validate the models used by the MC codes especially when the codes are used for charged particle therapy monitoring applications where high accuracy is required. In the meanwhile, the usage of external experimentally validated cross section as an alternative to the usage of the nuclear internal models of the codes is recommended.

Acknowledgments

This study was performed under the European collaboration ENVISION (Envision 2010) which focuses on the development of novel imaging modalities for (*in vivo*) dose monitoring and quality assurance of heavy charged particle therapy. It has been supported by the European FP7 project ENVISION (grant agreement no. 241851), the Foundation for Fundamental Research on Matter, The Netherlands (project no. 09NIG18–1) and the Bundesministerium für Bildung, Wissenschaft, Forschung und Technologie of Germany (grant 01IB08002F). JS is supported by the Belgian FNRS (aspirant). The authors are grateful to Alexey Stankovskiy (SCK-CEN, Mol, Belgium), Brigitte Reniers (Maastric Clinic, Maastricht, The Netherlands), Laurie Waters and Gregg W McKinney (LANL, Los Alamos, NM) for their valued advice on MCNPX simulations. The authors are also grateful to Guillaume Landry (Maastric Clinic, Maastricht, The Netherlands) for helpful suggestions regarding this paper.

Appendix.

Table A1. GEANT4 Opt3 parameters.

	GEANT4 Opt3		
	e^-/e^+	Proton	GenericIon
Stepping function—final range	0.1 mm	0.05 mm	0.02 mm
Stepping function—dRoverRange	0.2	0.2	0.1
Stepping algorithm	distanceToBoundary	–	–

Table A2. Models used in the GEANT4 simulations.

Hadronic process	Particles	Geant4 processes	Geant4 models	Geant4 data sets	Energy range
Elastic scattering	GenericIon	G4HadronElastic Process	G4LElastic	G4HadronElastic DataSet	–
	All other particles	G4UHadronElastic Process	G4HadronElastic	G4HadronElastic DataSet	–
Inelastic process for protons	Protons	G4ProtonInelastic Process	G4BinaryCascade	G4ProtonInelastic CrossSection	0–20 GeV
Inelastic process for ions	GenericIon	G4IonInelastic Process	G4BinaryLightIon Reaction	G4IonsShen Cross Section	0–20 GeV
	Deuteron, Triton, Alpha	G4IonInelastic Process	G4LEInelastic	G4TripathiLight CrossSection	0–80 MeV
			G4BinaryLightIon Reaction		80 MeV–20 GeV
Inelastic scattering for neutrons	Neutron	G4NeutronInelastic Process	G4NeutronHP Inelastic G4BinaryCascade	G4NeutronHP InelasticData G4NeutronInelasticCrossSection	0–20 MeV 14 MeV–20 GeV

References

- Agostinelli F *et al* 2003 GEANT4—a simulation toolkit *Nucl. Instrum. Methods Phys. Res.* **506** 250–303
- Andreo P 2009 On the clinical spatial resolution achievable with protons and heavier charged particle radiotherapy beams *Phys. Med. Biol.* **54** N205–15
- Armstrong T W and Chandler K C 1973 A Fortran program for computing stopping powers and ranges for muons, charged pions, protons and heavy ions ORNL-4869 *Oak Ridge National Laboratory*
- Attansi F, Knopf A, Parodi K, Paganetti H, Bortfeld T, Rosso V and Del Guerra A 2011 Extension and validation of an analytical model for in-vivo PET verification of proton therapy—a phantom and clinical study *Phys. Med. Biol.* **56** 5079–98
- Battistoni G, Muraro S, Sala P R, Cerutti F, Ferrari A, Roesler S, Fasso A and Ranft J 2007 The FLUKA code: description and benchmarking *Proc. Hadronic Shower Simulation Workshop 2006 (Fermilab, Sept. 2006)* 896 ed M Albrow and R Raja pp 31–49
- Beebe-Wang J, Vaska P, Dilmanian F A, Peggs S G and Schlyer D J 2003 Simulation of proton therapy treatment verification via PET imaging induced positrons emitters *Proc. IEEE Nucl. Sci. Symp. Conf. Rec.* vol 4 2496–500
- Bortfeld T 1997 An analytical approximation of the Bragg curve for therapeutic proton beams *Med. Phys.* **24** 2024–34
- Carlsson A K, Andreo P and Brahme A 1997 Monte Carlo and analytical calculation of proton pencil beams for computerized treatment plan optimization *Phys. Med. Biol.* **42** 1033–53
- Cerutti F, Battistoni G, Capezzali G, Colleoni P, Ferrari A, Gadioli E, Mairani A and Pepe A 2006 Low Energy nucleus–nucleus reactions: the BME approach and its interface with FLUKA *Proc. 11th Int. Conf. Nucl. React. Mechanisms (Varenna, Italy, June 2006)* Ric. Sci. Educ. Permanente (Supl. 126) 507–11 (http://www.mi.infn.it/~gadioli/Varenna2006/Proceedings/Cerutti_F.pdf)

- Chadwick M B, Young P G, Chiba S, Frankle S C, Hale Hughes H G, Koning A J, Little R C, MacFarlane R E, Prael R E and Waters L S 1999 Cross-section evaluations to 150 MeV for accelerator-driven systems and implementation in MCNPX *Nucl. Sci. Eng.* **131** 293–328
- Espana S, Zhu X, Daartz J, El Fakhri G, Bortfeld T and Paganetti H 2011 The reliability of proton-nuclear interaction cross-section data to predict proton-induced PET images in proton therapy *Phys. Med. Biol.* **56** 2687–98
- Envision 2010 <http://envision.web.cern.ch/ENVISION/>
- Ferrari A, Fasso A, Ranft J and Sala P R 2005 FLUKA: a multi-particle transport code CERN-2005–10 INFN /TC_05/11, SLAC-R-773
- Ferrari A and Sala P R 1998 The physics of high energy reactions *Proc. Workshop on Nucl. Reaction Data and Nucl. Reactors Physics, Design and Safety, ICTP (Trieste, April, 1996)* vol 2 ed A Grandini and G Reffo (Singapore: World Scientific) pp 424–532
- Furihata S 2000 Statistical analysis of light fragment production from medium energy proton-induced reactions *Nucl. Instrum. Methods B* **171** 251–8
- Grevillot L, Bertrand D, Dessy F, Freud N and Sarrut D 2011 A Monte Carlo pencil beam scanning model for proton treatment plan simulation using GATE/GEANT4 *Phys. Med. Biol.* **56** 2011 PMB 5203–21
- Grevillot L, Frisson L, Zahra N, Bertrand D, Stichelbaut F, Freud N and Sarrut D 2010 Optimization of GEANT4 settings for proton pencil beam scanning simulations using GATE *Nucl. Instrum. Methods Phys. Res. B* **268** 3295–305
- Herault J, Iborra N and Chauvel P 2005 Monte Carlo simulation of a proton therapy platform devoted to ocular melanoma *Med. Phys.* **32** 910–9
- ICRU 2000 Nuclear Data for Neutron and Proton Radiotherapy and for Radiation *ICRU Report No 63* (Bethesda, MD: ICRU)
- Iwase H, Niita K and Nakamura T 2006 Development of general-purpose particle and heavy ion transport Monte Carlo code *Radiat. Meas.* **41** 1080
- Jan *et al* 2011 GATE V6: a major enhancement of the GATE simulation platform enabling modeling of CT and radiotherapy *Phys. Med. Biol.* **56** 881–901
- Kimstrand P, Tilly N, Ahnesjö A and Traneus E 2008 Experimental test of Monte Carlo proton transport at grazing incidence in GEANT4, FLUKA and MCNPX *Phys. Med. Biol.* **53** 1115–29
- Mashnik S G 2006 Implementation of CEM03.01 into MCNP6 and its Verification and Validation Running Through MCNP6 CEM03.02 Upgrade X-3-RN(U)-07–03
- MCNPX 2002 MCNPX 2.3.0 User's Guide LA-UR-02–2607
- MCNPX 2008 MCNPX 2.6.0 Users's Guide 2008 LA-CP-07–1473
- MCNPX 2010 MCNPX 2.7.D Extensions, LA-UR-10–07031
- Nara Y, Otuka N, Ohnishi A, Niita K and Chiba S 2000 Relativistic nuclear collisions at 10 AGeV energies from p+Be to Au+Au with the hadronic cascade model *Phys. Rev. C* **61** 024901
- Niita K, Chiba S, Maruyama T, Takada H, Fukahori T, Nakahara Y and Iwamoto A 1995 Analysis of the (N,xN') reactions by quantum molecular dynamics plus statistical decay model *Phys. Rev. C* **52** 2620
- Nose H, Niita K, Hara M, Uematsu K, Azuma O, Miyauchi Y, Komori M and Kanai T 2005 Improvement of three-dimensional Monte Carlo code PHITS for heavy ion therapy *J. Nucl. Sci. Technol.* **42** 250
- Paganetti H and Gottschalk B 2003 Test of GEANT3 and GEANT4 nuclear models for 160 MeV protons stopping in CH2 *Med. Phys.* **30** 1926–31
- Paganetti H, Jiang H, Parodi K, Slopesma R and Engelsman M 2008 Clinical implementation of full Monte Carlo dose calculation in proton beam therapy *Phys. Med. Biol.* **53** 4825–53
- Parodi K and Enghardt W 2000 Potential application of PET in quality assurance of proton therapy *Phys. Med. Biol.* **45** N151–6
- Parodi K, Enghardt W and Haberer T 2002 In-beam PET measurements of β^+ -radioactivity induced by proton beams *Phys. Med. Biol.* **47** 21–36
- Parodi K *et al* 2007a Patient study of in vivo verification of beam delivery and range, using positron emission tomography and computed tomography imaging after proton therapy *Int. J. Radiat. Oncol.* **68** 920–34
- Parodi K, Ferrari A, Sommerer F and Paganetti H 2007b Clinical CT-based calculations of dose and positron emitter distributions in proton therapy using the FLUKA Monte Carlo code *Phys. Med. Biol.* **52** 3369–87
- Parodi K, Mairani A, Brons S, Naumann J, Sommerer F and Haberer T 2009 The application of the FLUKA Monte Carlo code to basic data generation for clinical treatment planning of scanned proton and carbon ion therapy *Book from Abstracts from European Workshop on Monte Carlo Treatment Planning (Cardiff, UK, 19–21 Oct.)* <http://www.mctp2009.org>

- Parodi K, Paganetti H, Cascio E, Flanz J B, Bonab A, Alpert N M, Lohmann K and Bortfeld T 2007c PET/CT imaging for treatment verification after proton therapy—a study with plastic phantoms and metallic implants *Med. Phys.* **34** 419–35
- Parodi K, Ponisch F and Enghardt W 2005 Experimental study on the feasibility of in-beam PET for accurate monitoring of proton therapy *IEEE Trans. Nucl. Sci.* **52** 778
- PHITS 2001 PHITS: particle and heavy ion transport code system JAERI-DATA/CODE 2010—22 Version 2.23
- Pshenichnov I, Mishustin I and Greiner W 2006 Distributions of positron-emitting nuclei in proton and carbon-ion therapy studied with GEANT4 *Phys. Med. Biol.* **51** 6099–112
- Rinaldi I, Ferrari A, Mairani A, Paganetti H, Parodi K and Sala P 2011 An integral test of FLUKA nuclear models with 160 MeV proton beams in multi-layer Faraday cups *Phys. Med. Biol.* **56** 4001–11
- Talys 2010 [ftp://ftp.nrg.eu/pub/www/talys/tendl2010/tendl2010.html](http://ftp.nrg.eu/pub/www/talys/tendl2010/tendl2010.html)
- Tripathi R K, Cucinotta F A and Wilson J W 1999 Accurate universal parametrization of absorption cross sections III—light systems *Nucl. Instrum. Methods B* **155** 349
- Sawakuchi G O *et al* 2010 An MCNPX Monte Carlo model of a discrete spot scanning proton beam therapy nozzle *Med. Phys.* **37** 4960–70
- Scheidenberger C and Geissel H 1998 Slowing down of relativistic heavy ions and new applications *Nucl. Instrum. Methods B* **136** 114
- Shen W Q, Wang B, Feng J, Zhan W L, Zhu Y T and Feng E P 1989 Total reaction cross section for heavy-ion collisions and its relation to the neutron excess degree of freedom *Nucl. Phys. A* **491** 130
- Stankovskiy A, Kerhoas-Cavata S, Ferrand R, Nauraye C and Demarzi L 2009 Monte Carlo modelling of the treatment line of the proton therapy center in Orsay *Phys. Med. Biol.* **54** 2377–94
- Waters L S 2010 private communication
- Zahra N, Frisson T, Grevillot L, Lautesse P and Sarrut D 2010 Influence of Geant4 parameters on dose distribution and computation time for carbon ion therapy simulation *Phys. Medica: Eur. J. Med. Phys.* **26** 202–8